PHYSICAL REVIEW A

GENERAL PHYSICS

THIRD SERIES, VOL. 7, NO. 2 FEBRUARY 1973

Angular Distribution of Bremsstrahlung from Mirror-Confined Electrons*

A. C. England and G. R. Haste
Oak Ridge National Laboratory, Oak Ridge, Tennessee 37830
(Received 26 July 1972)

The bremsstrahlung radiation from electron-ion collisions is emitted anisotropically in directions dependent on the electron kinetic energy and the photon energy. We consider here the radiation from electrons confined in magnetic mirrors. In particular, the magnitude of this anisotropy is examined as a function of the electron energy, the photon energy, the electron pitch angle, and the angle of a detector with respect to the magnetic-mirror midplane. The calculations are performed in the Born approximation with the cross sections developed by Gluckstern and Hull. We also compute the temperature of a bi-Maxwellian distribution from the slope of the log of the intensity vs photon-energy curve and consider the effects of pitch-angle distribution and detector angle on the anisotropy of the radiation.

I. INTRODUCTION

The bremsstrahlung radiation arising from electron-ion collisions is not emitted isotropically; rather it is emitted in preferred directions depending on the electron kinetic energy. In this paper we consider the consequences of this anisotropic emission on the bremsstrahlung from mirror-confined electrons. We assume that the radiation is emitted at random phases over the orbit of the electron and find the probability for detecting the resulting x rays at various angles with respect to the magnetic field.

Similar calculations using the nonrelativistic form of the bremsstrahlung cross section have been made by Shohet,[1] who showed that the x-ray spectra differed considerably when viewed parallel and perpendicular to the magnetic field. However, Shohet's calculations were based on the nonrelativistic Sommerfeld[2]–Kirkpatrick–Wiedmann[3] theory. The results given here generally apply to higher electron energies for which Shohet's calculations are not applicable. We make some specific comparisons at low temperature with Shohet's theory.

In this paper we show the magnitude of this anisotropy as a function of the electron and x-ray energies, of the electron pitch angle, and of the angle at which the detector is placed. We also calculate the temperature for bi-Maxwellian distributions from the slope of the intensity–vs–photon-energy curve. We show the effect of pitch-angle distributions and detector angle on this temperature.

II. CALCULATIONS

We have used the bremsstrahlung cross section given by Gluckstern and Hull[4] to find the relative probability of detecting the resultant x ray as a function of the detector angle at various electron pitch angles. The relativistic cross section is used, with different forms for "high" and "low" x-ray energies. This cross section neglects screening due to either bound or free electrons. We also neglect magnetic bremsstrahlung since for most laboratory plasmas this does not produce photons in the x-ray region. We have used a computer code to calculate this cross section; and, for the results quoted here for monoenergetic electrons, we have used the high-energy form of the cross section. It should be pointed out that the calculations of Gluckstern and Hull use the Born approximation, without the "Coulomb correction." Thus, the magnitude of the bremsstrahlung cross section is too low for x-ray energies which approach the electron kinetic energy. These calculations apply to a $Z=1$ plasma, so the neglect of screening effects is justified. However, the effects of electron-electron (e-e) bremsstrahlung are neglected, with less justification. At present

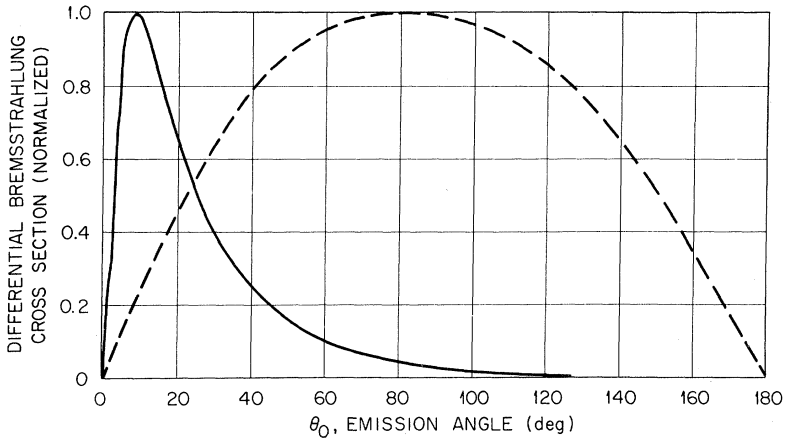

FIG. 1. Differential bremsstrahlung cross section vs emission angle. The solid curve is for $E_e = 1$ MeV; the dotted curve is for $E_e = 1$ keV. In each case $E_\gamma / E_e = 0.05$.

there are no formulations which can yield the angular distributions for e-e bremsstrahlung. Maxon[5] has shown that the magnitude of the e-e effect can be twice as great as the electron-ion effect at high electron temperatures ($kT_e \geq 1.5$ MeV).

Some investigations have shown discrepancies between the Born approximation and experiment. However, in a recent paper[6] calculations for $Z = 1$ show fairly good agreement (several percent) between more exact point Coulomb calculations and the Born approximation.

The differential cross sections for two electron energies are shown in Fig. 1. In this figure the cross sections are normalized to unity peak amplitude and are plotted against θ_0, the angle between the original electron direction and the x-ray direction. This figure illustrates the well-known "searchlight effect." The peak of the cross section is at 90° at low electron energies and moves toward the forward direction at high energies. If the electron motion is primarily perpendicular to the magnetic field, the radiation is enhanced parallel to the field for low-energy electrons and perpendicular for high-energy electrons.

To make these considerations more quantitative, we have defined a "relative detection probability $P(\psi)$" as a function of the detector angle ψ. This is defined such that, if the bremsstrahlung *were* isotropic, $P(\psi)$ would be unity and independent of ψ. To the extent that the radiation is enhanced in a direction ψ, the probability $P(\psi)$ is greater than unity. The geometry used for calculating $P(\psi)$ is shown in Fig. 2. The electron has a pitch angle α with respect to the midplane, the detector lies in the xz plane at an angle ψ with respect to the midplane, the phase angle of the electron in its orbit is β, and the angle between the x-ray direction and the electron velocity is θ_0. Since these electrons are mirror confined, for each electron with a pitch angle α, there is also an electron with pitch angle $-\alpha$.

We define $P(\psi)$,

$$P(\psi) = \frac{\int_0^{2\pi} d\sigma\,[E_e, E_\gamma, \alpha, \psi, \theta_0(\beta)]\,d\beta + \int_0^{2\pi} d\sigma\,[E_e, E_\gamma, -\alpha, \psi, \theta_0(\beta)]\,d\beta}{\int_0^{\pi/2} d\psi \cos\psi \left[\int_0^{2\pi} d\sigma(E_e, E_\gamma, \alpha, \psi, \theta_0)\,d\beta + \int_0^{2\pi} d\sigma(E_e, E_\gamma, -\alpha, \psi, \theta_0)\,d\beta\right]},$$

where E_e is the electron kinetic energy, E_γ is the x-ray energy, and $d\sigma$ is the differential bremsstrahlung cross section.

The denominator of the expression is proportional to the total probability of emission and $P(\psi)$ is the relative probability that the x-ray will be emitted between ψ and $\psi + d\psi$. Implicit in this expression is the assumption that the emission is independent of the phase angle β, about the axis of symmetry provided by the magnetic field.

III. RESULTS FOR SINGLE ELECTRONS

We will show several angular distributions $P(\psi)$ for various electron energies and pitch angles, all for unique values of these parameters. In succeeding sections we show the consequences of having a distribution in these parameters.

All of the distributions $P(\psi)$ are normalized to the same area using the denominator of Eq. (1). This normalization factor is obtained by integrating the differential cross section over all solid angles and is thus proportional to the integrated cross section. The variation of this factor with x-ray energy can be used to check the validity of the calculation. Figure 3 shows this variation. The solid curve shows the integrated bremsstrahlung cross section as a function of the photon energy, as given by Heitler.[7] The points are calculated values with

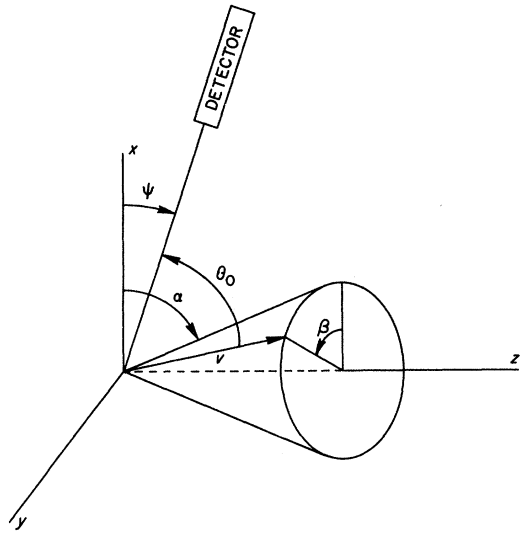

FIG. 2. Geometry used for calculating $P(\psi)$.

the point $E_\gamma/E_e = 0.65$ fitted to the curve. It appeared that the agreement was sufficient.

There are two significant angles: the pitch angle of the electron α and the detector angle ψ. In Fig. 4 we show $P(\psi)$ for a pitch angle of 0°, for two electron energies, 10 and 100 keV. At the low energy the radiation is primarily normal to the electron motion, so $P(\psi)$ is peaked in the direction of the magnetic field. At 100 keV the radiation is nearly isotropic and $P(\psi) \approx 1$ for all ψ. Figure 5 shows the same plot at 1 MeV, and for various x-ray energies. At energies this high the radiation is strongly peaked in the forward direction and $P(\psi)$ is strongly peaked for small ψ. Note that the variation of $P(\psi)$ with the x-ray energy is relatively small. We will ignore this variation in what follows.

The other variation of interest is with the electron pitch angle. Figure 6 shows this variation for an electron of 1 MeV and for an x-ray energy of 650 keV. The principal effect shown in Fig. 6 is that electrons with small pitch angles concentrate

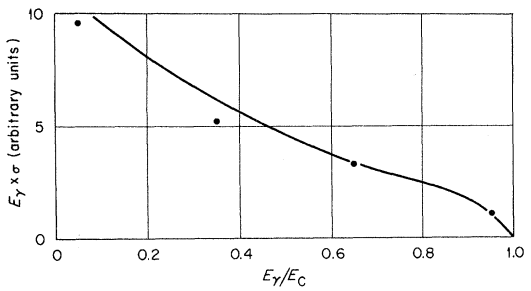

FIG. 3. Comparison of integrated cross section (dots) with that of Heitler (solid curve).

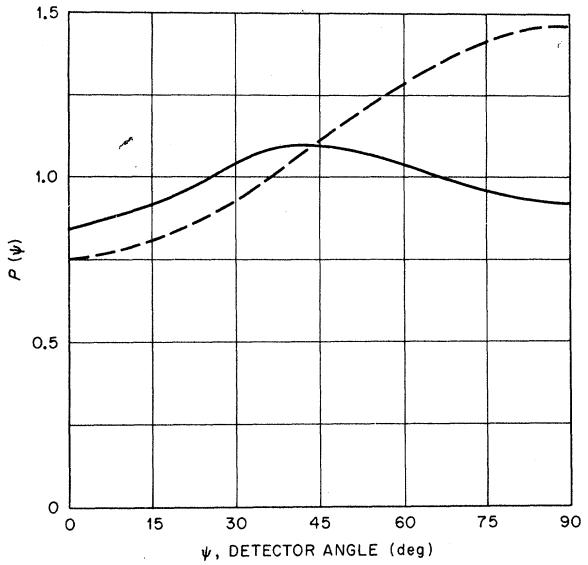

FIG. 4. $P(\psi)$ vs ψ. For the dotted curve $E_e = 10$ keV; for the solid curve $E_e = 100$ keV. In each case $E_\gamma/E_e = 0.65$.

their radiation at small ψ, that is, near the midplane. As the pitch angle is increased the radiation becomes more isotropic in that the peak height is

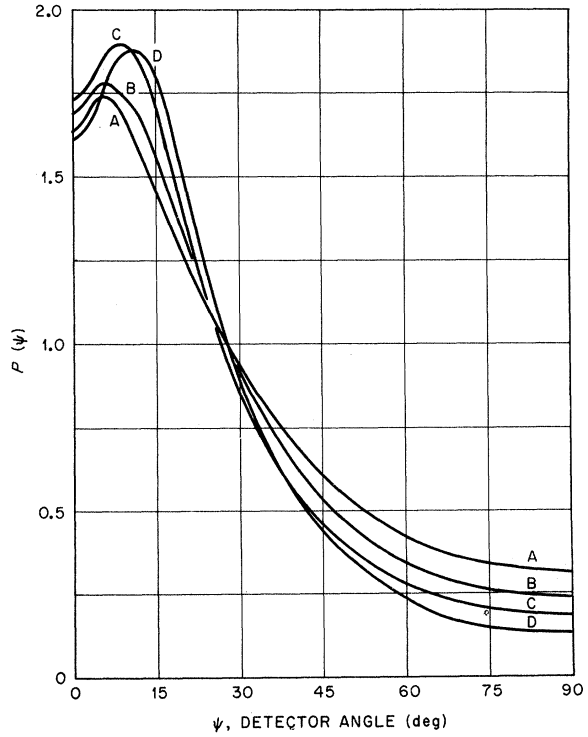

FIG. 5. $P(\psi)$ vs ψ for various x-ray energies, $E_e = 1$ MeV. A, $E_\gamma = 50$ keV; B, $E_\gamma = 350$ keV; C, $E_\gamma = 650$ keV; D, $E_\gamma = 950$ keV.

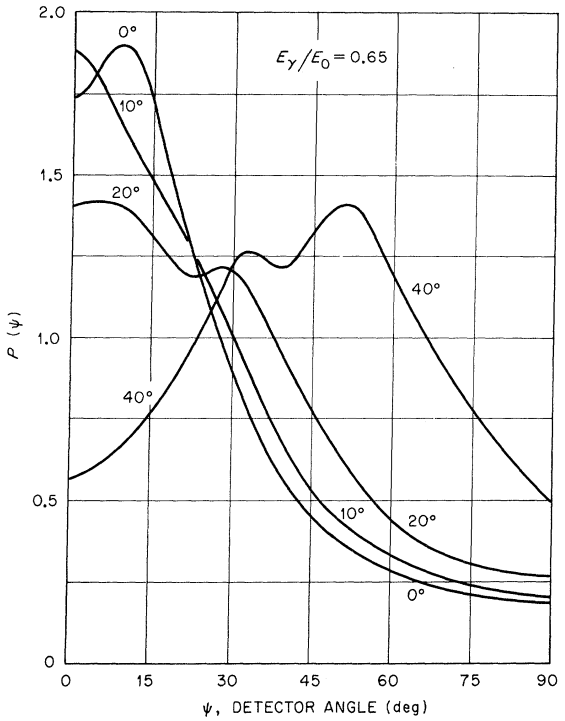

FIG. 6. $P(\psi)$ vs ψ for various pitch angles, E_e=1 MeV.

reduced and the peak width is increased. At lower energies the radiation is nearly isotropic even for 0° pitch angles, so the change in isotropy is small. At higher energies the differential cross section is so large in the forward direction that the resulting $P(\psi)$ is sharply peaked for $\psi \approx \alpha$, as shown in Fig. 7, for 3-MeV electrons. This effect masks the variation of the isotropy with α.

IV. RESULTS FOR MONOENERGETIC ELECTRONS WITH INTEGRATION OVER PITCH ANGLE

An integration over a range of pitch angles was used to investigate the bremsstrahlung radiation pattern, i.e., $P(\psi)$ vs ψ. Several electron energies were used and the normalization was carried out as before. We use here the usual definition of mirror ratio in terms of the loss cone. For small mirror ratios, the pitch-angle range is small and vice versa. In particular the relation between the mirror ratio R and the maximum pitch angle α_{max} is given by $\cos\alpha_{max} = 1/\sqrt{R}$.

For an electron kinetic energy of 1 MeV and an isotropic distribution, i.e., pitch angles from 0° to +90°, there is no variation in $P(\psi)$. For $0° \leq \alpha \leq +60°$, i.e., a ~ 4:1 mirror, Fig. 8 shows modest peaking on the midplane. For a smaller range of pitch angles (a lower mirror ratio), the peaking is more predominant, as would be expected.

For an intermediate energy electron, 0.1 MeV, and the same ranges of pitch angles, Fig. 9 shows the results. Here the distribution in ψ is quite flat and there is a very minor increase at $\psi = 90°$ for a mirror ratio of 4:1 with a very slight intermediate dip. Changing the mirror ratio has a very small effect because the low-energy photon distribution is almost isotropic.

V. RESULTS FOR BI-MAXWELLIAN DISTRIBUTION FUNCTION

A. Angular Distributions

We show here a set of graphs showing the effect of a change of mirror ratio with an isotropic plasma contained up to the pitch-angle limit imposed by the mirror ratio and also an anisotropic plasma in a given mirror. We have used an anisotropic or two-temperature Maxwellian distribution function

$$f \propto \sqrt{E_e} \exp\left[-\frac{E_e}{\theta mc^2}\left(\cos^2\alpha + \frac{1}{T}\sin^2\alpha\right)\right],$$

where θmc^2 is the electron temperature in MeV, E_e is the electron kinetic energy in MeV, and the anisotropy parameter $T = \theta_{\parallel}/\theta_{\perp}$ (small values of T are more anisotropic). Note here that the distribution function f is defined so that the number of particles in an energy-angle interval is given by

$$dN = 2\pi f dE \cos\alpha \, d\alpha.$$

Note also that the average particle energy is given by

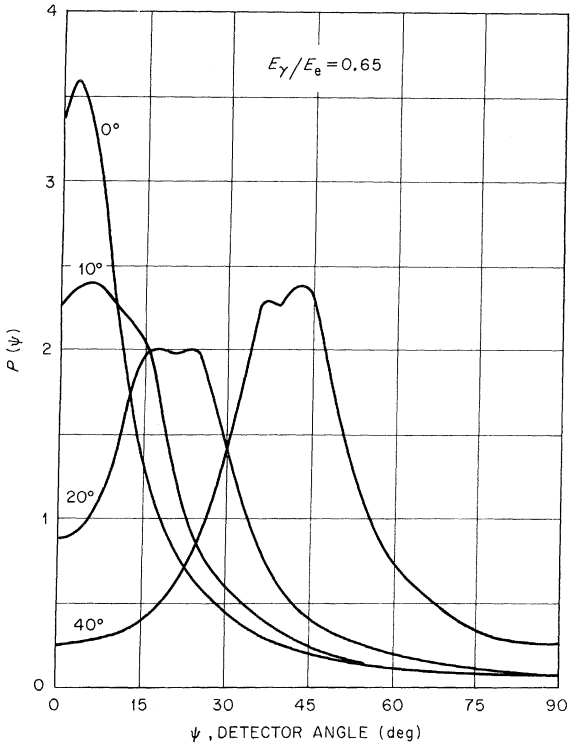

FIG. 7. $P(\psi)$ vs ψ for various pitch angles, E_e=3 MeV.

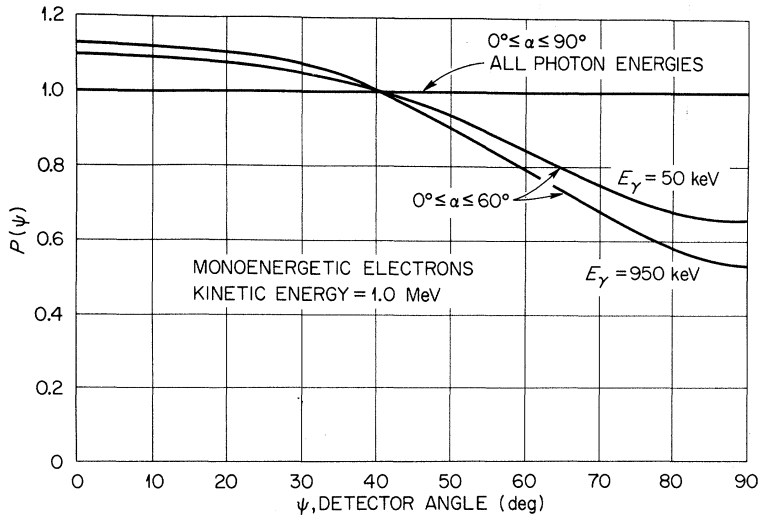

FIG. 8. $P(\psi)$ vs ψ for 1-MeV electron energy and two photon energies. Pitch angles between 0° and +60°; a 4:1 mirror ratio.

$\overline{E} = \frac{1}{2}\,\theta mc^2(2+T)$.

We always took an upper limit of 6 MeV on the electron energy. (This upper limit is typical of electron-cyclotron plasmas in the ELMO[8] mirror facility, for example. This limit is somewhat too high for other facilities employing electron-cyclotron heating, e.g., IMP and INTEREM.[9] We have used this distribution function because it is well known and widely used. However, it is not necessarily representative of actual mirror-confined distributions.

Figure 10 shows the dependence of $f(E_e, \alpha)$ on pitch angle for various anisotropies. For a nonrelativistic Maxwellian, the solid curves show that the smaller T (the more anisotropic), the narrower the distribution becomes in pitch angle. All the curves are independent of the electron energy. The question arises as to whether we could simplify the distribution function further by replacing this anisotropic Maxwellian distribution function with an isotropic version ($T = 1$ always) and integrate over a smaller range of pitch angles, i.e., replace the anisotropic distribution in a given mirror with an isotropic distribution in a smaller mirror. We will see the effect of this replacement later.

The next two graphs, Figs. 11 and 12, show the angular distribution of the radiation for two different temperatures and anisotropies of $T = 1$ and $T = 0.2$.

Figure 11 shows that at high temperatures $\theta = 3$ ($\theta mc^2 = 1.53$ MeV) and at high photon energies the angular distribution indicates fairly accurately the electron-pitch-angle distribution. (For $T = 1$, the pitch-angle distribution would be flat out to 45° and zero beyond that in a 2:1 mirror.) For a

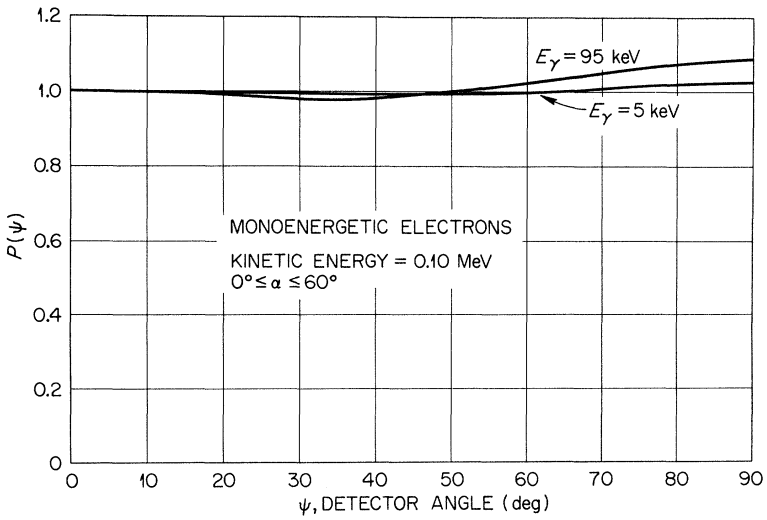

FIG. 9. $P(\psi)$ vs ψ for 100-keV electron energy and two photon energies. Pitch angles between 0° and +60°; a 4:1 mirror ratio.

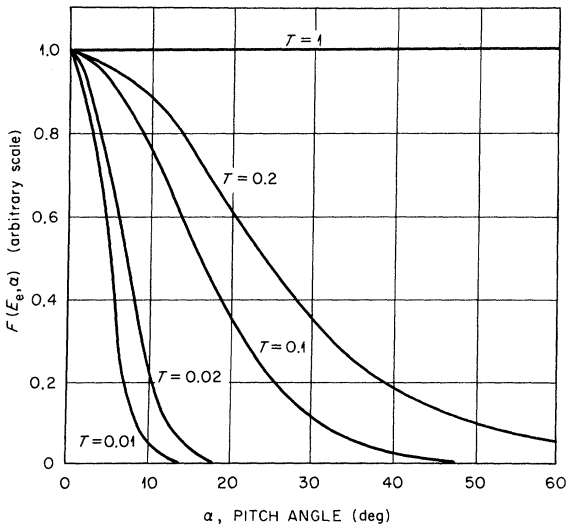

FIG. 10. Behavior of an anisotropic Maxwellian distribution function as a function of the electron pitch angle.

higher mirror ratio ($\alpha_{max} > 45°$) the plateau region of the angular distribution is wider.

For $T = 0.2$ (an anisotropic plasma) the full width at half-maximum (FWHM) of the x-ray angular distribution is much narrower, as is seen in Fig. 12, but nevertheless the distribution at high photon energies represents rather well the electron-pitch-angle distribution (cf. Fig. 10). The FWHM is several tens of degrees wide even at the highest photon energy plotted. This means that small misalignments in collimators would not make serious errors in the intensity and temperature measurement unless we had a much more anisotropic plasma or a very low mirror ratio. Figure 13 shows an angular distribution for a lower temperature.

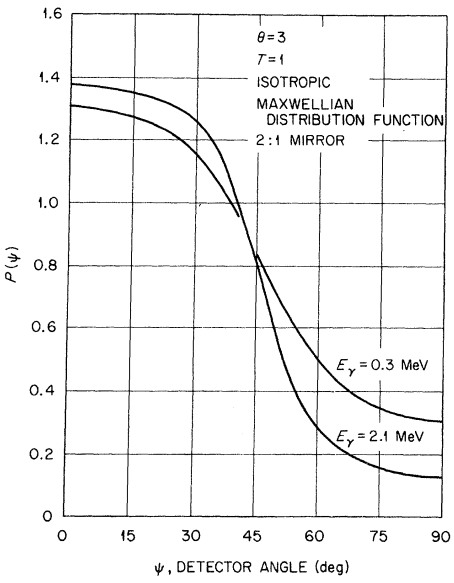

FIG. 11. $P(\psi)$ vs ψ for an isotropic Maxwellian in 2:1 mirror, $\theta mc^2 = 1.53$ MeV.

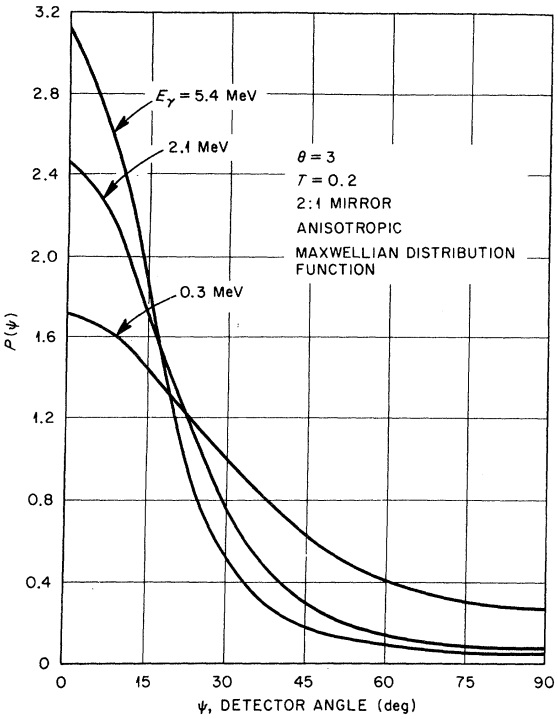

FIG. 12. $P(\psi)$ vs ψ for an anisotropic Maxwellian in 2:1 mirror, $\theta mc^2 = 1.53$ MeV.

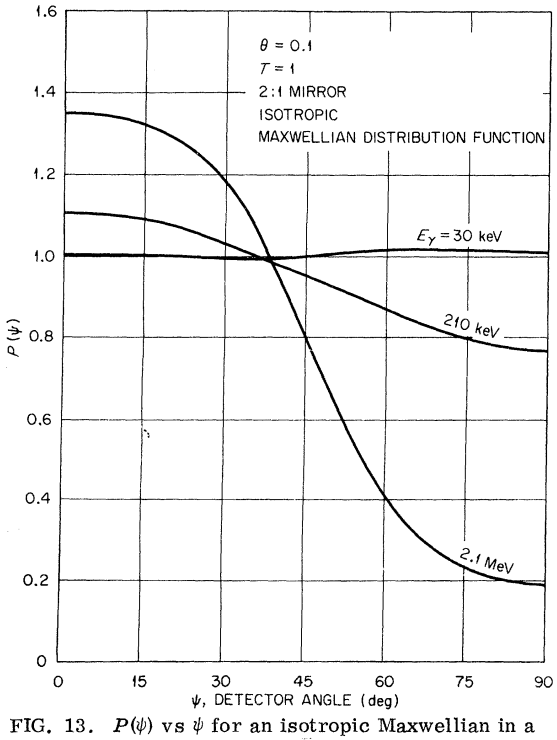

FIG. 13. $P(\psi)$ vs ψ for an isotropic Maxwellian in a 2:1 mirror, $\theta mc^2 = 51.1$ keV.

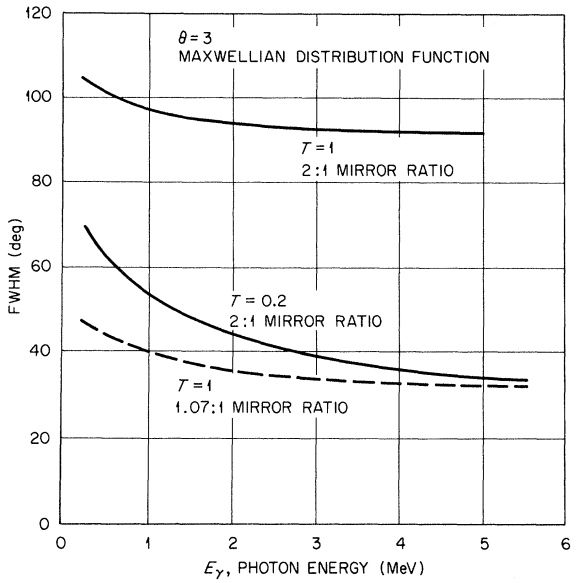

FIG. 14. FWHM vs photon energy for isotropic and anisotropic Maxwellians in a 2:1 and 1.07:1 mirror, $\theta mc^2 = 1.53$ MeV.

Note that at very low photon energies there is slight peaking near $\psi = 90°$. We have used here the low-photon-energy approximation for the cross section given in Ref. 4.

Figure 14 shows the width (FWHM) of the x-ray angular distribution for a Maxwellian distribution contained in a mirror ratio of 2:1. The electron distribution is characterized by a temperature of 1.53 MeV and one of two pitch-angle distributions: The first has an anisotropy parameter $T = 1$ such that the pitch-angle distribution is flat out to 45°; the second has $T = 0.2$ such that most of the particles have small pitch angles. In the first case ($T = 1$) and at high photon energies, the width of the radiation distribution reflects the width of the pitch-angle distribution, since both are 90°. In the second case ($T = 0.2$) the width of the radiation distribution at high photon energy tends toward 35°, which is close to the width expected for single electrons at zero pitch angle.

If, as suggested earlier, we replace the anisotropic distribution with an isotropic distribution with a pitch-angle range from 0° to 25° [corresponding to the half-value of $f(E_0, \alpha)$ for $T = 0.2$ in Fig. 10], the resulting curves are much broader. In other words, the FWHM does not in this case resemble the anisotropic distribution FWHM.

We can take a smaller pitch-angle range, 0°–15° ($R = 1.07:1$), corresponding to ~0.78 of the maximum value of $f(E_0, \alpha)$ for $T = 0.2$ in Fig. 10, and we find at high photon energies the FWHM tends to be about the same value as the anisotropic case. However, comparison of the curves of $P(\psi)$ vs ψ show that even though the FWHM's are the same, the isotropic distribution with the smaller pitch-angle range displays much steeper sides than the anisotropic distribution with the larger pitch-angle range. Hence we cannot justify simplifying the calculation by using this technique to approximate an anisotropic distribution function. This observation suggests that the functional dependence on α of the electron distribution might be determined from a measure of the shape of $P(\psi)$ vs ψ.

In Fig. 15 we show the effects of increased anisotropy on the FWHM for two photon energies. Note that there is an apparent leveling off of the FWHM at high anisotropy (small values of T) for both of the photon energies shown. The higher-photon-energy curve levels off more quickly and the asymptotic value is just that expected for the width of the radiation pattern produced by the highest-energy electrons in the distribution.

In Fig. 16 we show the FWHM as a function of electron temperature for a nonrelativistic Maxwellian in a 2:1 mirror. Somewhat surprisingly, at relatively high photon energies the FWHM for an anisotropic plasma may either decrease or rise as the temperature θ increases. Figure 17 shows the variation of the FWHM with inverse mirror ratio for two photon energies. A plot of the maximum pitch angle contained in a mirror vs the inverse mirror ratio [$2\alpha_{max} = 2\arccos(R)^{-1/2}$] is also plotted for comparison to show that the FWHM is always larger than $2\alpha_{max}$ but does follow its trend.

The higher-photon-energy curve ($E_\gamma = 5.4$ MeV) more closely follows the curve of $2\alpha_{max}$, while the lower-energy curve ($E_\gamma = 0.3$ MeV) shows more broadening. For $R = 1$ the higher-energy curve intercepts the ordinate at ~15°, while the lower-energy curve intercepts the ordinate at ~35°. Note that these values are about the same as the asymptotic values of the FWHM in Fig. 15 for small val-

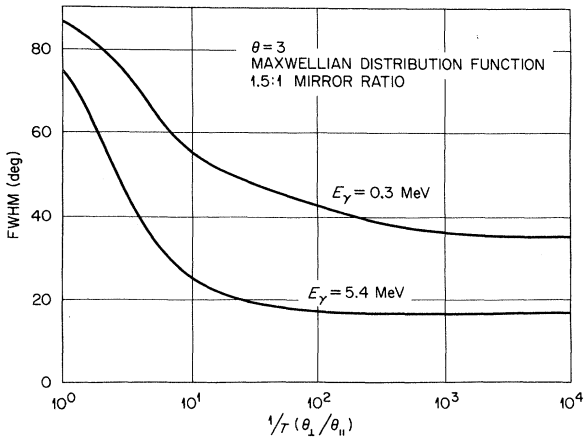

FIG. 15. FWHM vs $1/T$ for Maxwellian in a 2:1 mirror, $\theta mc^2 = 1.53$ MeV.

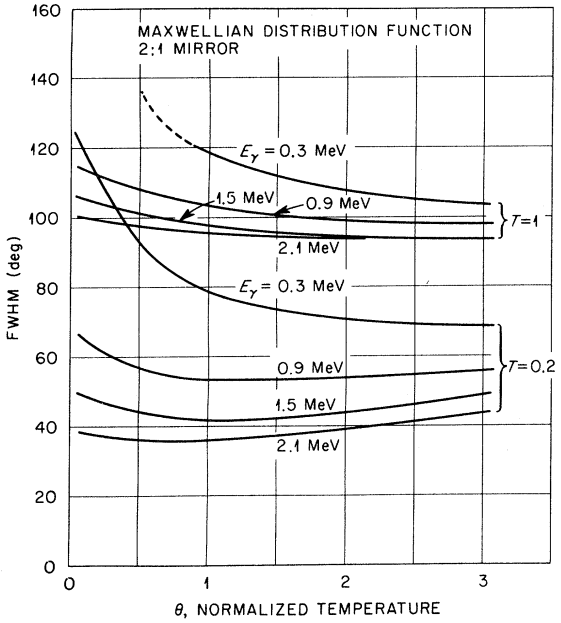

FIG. 16. FWHM vs θ for isotropic and anisotropic Maxwellians.

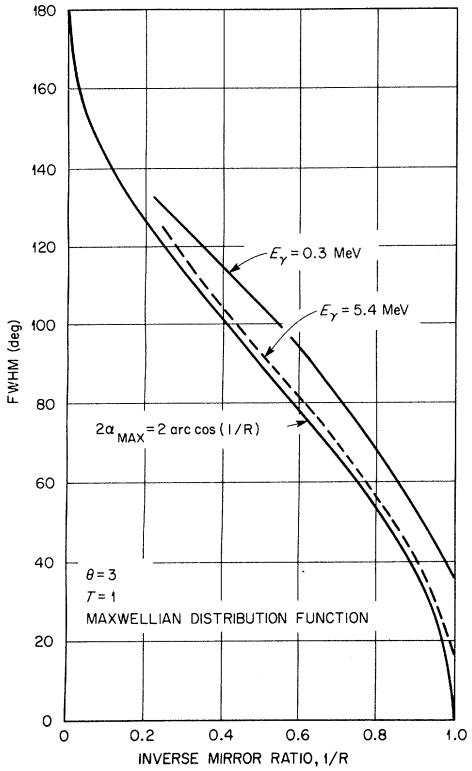

FIG. 17. FWHM vs $1/MR$ for isotropic Maxwellians with $\theta mc^2 = 1.53$ MeV.

ues of T, indicating that these are the inherent minimum widths of the curves.

B. Temperature Determinations

A nonrelativistic calculation can be made which shows that the slope of the log of the intensity vs photon energy is inversely proportional to the temperature.[8] Figure 18 shows the intensity of the radiation on an arbitrary scale as a function of the photon energy for two detector angles, $\psi = 0°$ and $\psi = 90°$, and for two different anisotropies. The intensity is proportional to the photon energy times the unnormalized probability of emission. Note that there is no single slope to the curve. In fact, the smallest value of the slope gives a maximum temperature of the order of but somewhat less than θmc^2. The increased slope at the low-photon-energy end is due to an increase in the cross section (cf. Fig. 3). The increased slope at the high-photon-energy end is due to our arbitrary cutoff in the electron energy which we have imposed on the distribution. Raising this limit decreases the slope. However, in most machines there is a practical limit to the electron energy that can be contained so that this effect is to be expected.

The agreement between the slope of the intensity curve and the temperature for a Maxwellian distribution is best for detector angles near $\psi = 0°$. The minimum discrepancy is ~6% for $\psi = 0°$ and occurs at the lowest temperatures. The maximum discrepancy for $\psi = 0°$ is ~30% at the highest temperature examined. The discrepancy would be even larger at higher temperatures. The agreement is worse at larger detector angles, particularly when the detector angle is greater than the maximum con

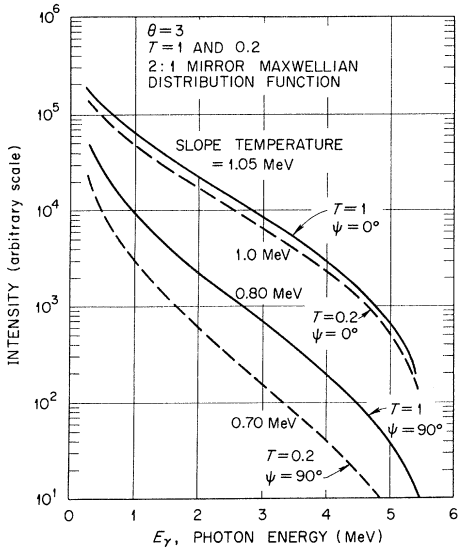

FIG. 18. Log of the intensity vs photon energy for isotropic Maxwellian distribution functions in 2 : 1 mirror, $\theta mc^2 = 1.53$ MeV.

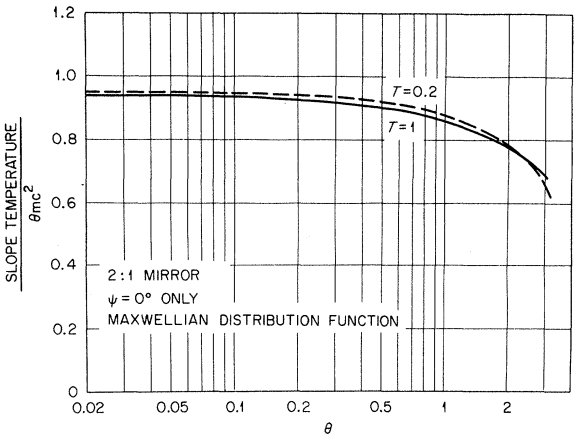

FIG. 19. Normalized minimum slope of the log of the intensity as function of normalized temperature θ, for isotropic and anisotropic plasmas.

tained pitch angle. The limiting value is obtained for a high-temperature highly anisotropic plasma, viewed with a detector angle of $\psi = 90°$. In that case, the "slope temperature" is ~70% of the temperature at $\psi = 0°$. In no case is the "slope temperature" greater than the true temperature.

The results in this paper are in disagreement with those of Shohet,[1] where a nonrelativistic treatment was used. In that work, the electron temperature calculated for $\psi = 90°$ was higher than for $\psi = 0°$. This difference is apparently due to the inclusion of relativistic effects in the Gluckstern–Hull[4] treatment. A recent paper by Greene and Shohet[10] confirms this.

The cross section used in this work does not include the "Coulomb correction" (or Elwert) factor. However, since this factor is not a strong function of ψ,[11] one would not expect its inclusion to have much effect on the angular distribution of the bremsstrahlung.

Figure 19 shows the minimum slope of the intensity–vs–photon-energy curve as a function of the normalized temperature θ. We conclude that the slope of the bremsstrahlung intensity-vs-energy curve remains a fairly good indication of the temperature as long as the temperature is much less than the maximum electron energy. As mentioned earlier, the drop off at high values of θ is due to the electron kinetic energy cutoff at 6.0 MeV. However, the slope at low values of θ is little affected by this cutoff and for a Maxwellian remains slightly below the value of θ.

Finally, we have examined the effects of both mirror ratio and anisotropy on the ratio of the measured "temperature" to θmc^2. We found a slight intermediate minimum both as a function of T and of R for $\theta = 3$ and $\psi = 0°$. It appears that the measured temperature is neither a strong function nor a monotonic function of either of these parameters.

It should be noted that the determination of "temperature" from the slope of the intensity–vs–photon-energy curve does not imply that the distribution is Maxwellian. For instance, a monoenergetic mirror-contained distribution of electrons will also produce a photon spectrum. Over some energy interval, the intensity will display an approximately linear decrease with photon energy on a logarithmic scale. For these distributions, the "temperature" found from this minimum slope is roughly one-half of the kinetic energy of the electrons.

It follows that many other distributions would give rise to intensity spectra from which one could determine a "temperature." The "temperature" so determined is clearly not related to a Maxwellian electron distribution and does not imply random velocities, but nevertheless can be used to find a mean or suitably averaged electron energy for the distribution producing the radiation. This effect has been noted previously.[12]

VI. CONCLUSIONS

This study of the angular distribution of bremsstrahlung from mirror-confined electrons has shown two features. First, the effective solid angle for detecting x rays from these electrons is a function of their energy and pitch angle as well as the detector angle, and the magnitude of this effect has been shown.

For mirror-confined Maxwellian distributions of electrons, there is generally found a peaking of the radiation on the midplane, and this effect is more pronounced for high temperatures, high photon energies, and more anisotropic distributions. For low photon energies and low temperatures, there can be a peaking along the field direction.

The study has also shown that for the distributions studied here the measured temperature is generally slightly lower than the temperature of the Maxwellian giving rise to the radiation. At high temperatures this can represent an error of ~30%, mostly due to the upper limit on the electron energy imposed by the experiment or the calculation. Again, owing to statistical errors and necessary corrections to data obtained from pulse-height spectra, errors of this magnitude may normally appear. Measurements of temperature for detectors at an angle to the midplane may give a lower value than measurements on the midplane.

ACKNOWLEDGMENTS

The authors would like to thank R. A. Dandl for having suggested the problem. Discussions with Owen Eldridge and other members of the Thermonuclear Division are gratefully acknowledged. The dedicated assistance of Eric Ferguson in programming the problem was invaluable to the authors.

*Research sponsored by the U. S. Atomic Energy Commission under contract with the Union Carbide Corp.

[1]J. L. Shohet, Phys. Fluids 11, 1065 (1968).
[2]A. Sommerfeld, *Atombau und Spectrallinien* (Vieweg, Braunschweig, Germany, 1951).
[3]P. Kirkpatrick and L. Wiedmann, Phys. Rev. 67, 321 (1945).
[4]R. L. Gluckstern and M. H. Hull, Jr., Phys. Rev. 90, 1030 (1953).
[5]S. Maxon, Phys. Rev. A 5, 1630 (1972).
[6]H. K. Tseng and R. H. Pratt, Phys. Rev. A 3, 100 (1971).
[7]W. Heitler, *The Quantum Theory of Radiation* (Oxford U. P., London, 1950), p. 170, Fig. 14.
[8]R. A. Dandl *et al.*, Nucl. Fusion 4, 344 (1964).
[9]W. B. Ard *et al.*, in *Plasma Physics and Controlled Nuclear Fusion Research* (International Atomic Energy Agency, Vienna, 1971), Vol. II, p. 619.
[10]D. G. S. Greene and J. L. Shohet, Plasma Phys. (to be published).
[11]G. Elwert and E. Haug, Phys. Rev. 183, 90 (1969).
[12]A. J. Lichtenberg *et al.*, Plasma Physics 13, 89 (1971).

PHYSICAL REVIEW A VOLUME 7, NUMBER 2 FEBRUARY 1973

Use of Furry-Sommerfeld-Maue Wave Functions in Pair Production and Bremsstrahlung*†

J. K. Fink‡§ and R. H. Pratt
Department of Physics, University of Pittsburgh, Pittsburgh, Pennsylvania 15123

(Received 19 June 1972; revised manuscript received 10 October 1972)

An analytic expression for the differential pair-production cross section is obtained using full Furry–Sommerfeld–Maue wave functions for the electron and positron. It is shown that this expression reduces to the Bethe–Maximon approximation and the Born approximation in the appropriate limits, and that it goes into the corresponding Elwert–Haug approximation for bremmstrahlung via the substitution rule. It is found that the cross sections of the Born approximation and the Bethe–Maximon approximation may be related to the cross section of the present approximation by a normalization theory similar to that used to relate point-Coulomb and screened "exact" calculations for pair production. No such theory works for bremsstrahlung because a larger-r region is of importance in the bremsstrahlung process. The region of validity of each approximation is found by comparison with "exact" numerical calculations. There exists a region of low energies and small Z where the present theory for pair production and the Elwert–Haug approximation for bremsstrahlung are valid and are significantly better than the Born and the Bethe–Maximon approximations. The failure of these calculations at low energies for intermediate and high Z is attributed to the fact that the lowest partial waves for the electron and positron, which are dominant at low energies, are very poorly represented in the Furry–Sommerfeld–Maue approximation.

I. INTRODUCTION

Furry–Sommerfeld–Maue wave functions have long been used in the calculation of cross sections for pair production and bremsstrahlung.[1] Their best-known application is due to Bethe and Maximon,[2] who argued that the wave functions are correct when $a^2/|\kappa| \ll 1$ and used them to calculate high-energy approximations to pair production and bremsstrahlung. Here $a \equiv Ze^2$, with e^2 as the fine-structure constant and $j = |\kappa| - \frac{1}{2}$ is the angular momentum of a partial wave in the expansion of the wave function. In addition to the approximations made in the derivation of Furry–Sommerfeld–Maue wave functions, together with the omission of a term in the matrix element which is small of relative order a, Bethe and Maximon made two further assumptions in their calculation of the matrix elements. The first assumption was that of high energy, enabling them to drop terms $O(1/E^2)$ and $O(1/k^2)$ compared to unity,[3] where E is the energy of either fermion and k is the photon energy. Second, they assumed that the angles between the photon and either fermion are small, since at high energies the main contribution to the cross section for pair production and bremsstrahlung is from near the forward direction. These assumptions simplified the expression for the totally differential cross section so that it could be integrated analytically over angles to obtain an expression for the cross-section differential only in energy.[4]

Bethe and Maximon showed that the Furry–Sommerfeld–Maue wave function ψ_{sm} satisfies the second-order Dirac equation to terms $O(a^2/|\kappa|)$. They also obtained ψ_{sm} from Darwin's partial-wave series solution of the more restrictive first-order Dirac equation by neglecting terms $O(a^2/|\kappa|)$ in each term of the series and summing the infinite series; this approach has also been discussed by Johnson and Deck.[5] The neglect of terms $O(a^2/|\kappa|)$ in the wave function leads to errors $O(a/|\kappa|)$ in the cross section, because the lowest-order term in the matrix element is not $O(1)$ as in the wave function but $O(a)$ (energy and momentum conservation forbid the processes in the absence of